

Discovery of a Novel Nonphosphorylated Pentapeptide Motif Displaying High Affinity for Grb2-SH2 Domain by the Utilization of 3'-Substituted Tyrosine Derivatives

Yan-Li Song,[†] Megan L. Peach,[‡] Peter P. Roller,[§] Su Qiu,^{||} Shaomeng Wang,^{||} and Ya-Qiu Long^{†,*}

State Key Laboratory of Drug Research, Shanghai Institute of Materia Medica, Shanghai Institutes for Biological Sciences, Graduate School of the Chinese Academy of Sciences, Chinese Academy of Sciences, 555 Zuchongzhi Road, Shanghai 201203, China, Basic Research Program, SAIC-Frederick, Inc., National Cancer Institute at Frederick, 376 Boyles Street, Frederick, Maryland 21702, Laboratory of Medicinal Chemistry, National Cancer Institute, National Institutes of Health, 376 Boyles Street, Frederick, Maryland 21702-1201, and University of Michigan Comprehensive Cancer Center, Departments of Internal Medicine and Medicinal Chemistry, University of Michigan, Ann Arbor, Michigan 48109-0934

Received September 14, 2005

The growth factor receptor-bound protein 2 (Grb2) is an SH2 domain-containing docking module that represents an attractive target for anticancer therapeutic intervention. An impressive number of synthetic Grb2-SH2 domain inhibitors have been identified; however, clinical agents operating by this mechanism are lacking, due in part to the unique requirement of anionic phosphate-mimicking functionality for high SH2 domain-binding affinity or the extended peptide nature of most inhibitors. In the current study, a new binding motif was successfully developed by the incorporation of 3'-substituted tyrosine derivatives into a simplified nonphosphorylated cyclic pentapeptide scaffold (**4**), which resulted in high affinity Grb2-SH2 inhibitors without any phosphotyrosine or phosphotyrosine mimetics. The new L-amino acid analogues bearing an additional nitro, amino, hydroxy, methoxy or carboxy group at the 3'-position of the phenol ring of tyrosine were prepared in an orthogonally protected form suitable for solid-phase peptide synthesis using Fmoc protocols. The incorporation of these residues into cyclic peptides composed of a five-amino acid sequence motif, Xx¹-Leu-(3'-substituted-Tyr)-Ac6c-Asn, provided a brand new class of nonphosphorylated Grb2 SH2 domain inhibitors with reduced size, charge and peptidic character. The highest binding affinity was exhibited by the 3'-aminotyrosine (3'-NH₂-Tyr)-containing (*R*)-sulfoxide-cyclized pentapeptide (**10b**) with an IC₅₀ = 58 nM, the first example with low-nanomolar affinity for a five-amino acid long sequence binding to Grb2-SH2 domain free of any phosphotyrosine or phosphotyrosine mimics. However, the incorporation of 3'-NO₂-Tyr, 3'-OH-Tyr or 3'-OCH₃-Tyr surrogates in the pentapeptide scaffold is detrimental to Grb2-SH2 binding. These observations were rationalized using molecular modeling. More significantly, the best Grb2-SH2 inhibitor **10b** showed excellent activity in inhibiting the growth of erbB2-dependent MDA-MB-453 tumor cell lines with an IC₅₀ value of 19 nM. This study is the first attempt to identify novel nonphosphorylated high affinity Grb2 SH2 inhibitors by the utilization of 3'-substituted tyrosine derivatives, providing a promising new strategy and template for the development of non-pTyr-containing Grb2-SH2 domain antagonists with potent cellular activity, which potentially may find value in chemical therapeutics for erbB2-related cancers.

Introduction

The Src homology 2 (SH2) domain is the most prevalent protein binding module that recognizes phosphotyrosine. By means of binding to specific phosphotyrosine-containing protein sequences, SH2 domains control intracellular signaling events.^{1,2} Among the SH2 domains, the growth factor receptor-bound protein 2 (Grb2) family directly mediates erbB-2 (HER-2/neu) signaling and the downstream activation of mitogenic Ras pathways, which have been implicated in the etiology of certain breast cancers.^{3,4} Compounds which selectively antagonize the Grb2-SH2 domain should interrupt these signaling pathways and thus are attractive targets for drug therapy in oncology.^{5–7} Recent papers reported significant advances in the use of "SH2 domain signaling antagonists" in cancer therapy and osteoporosis;^{8–11} however, clinical agents operating by this mechanism are lacking, due in part to the unique requirement of

anionic phosphate-mimicking functionality for high SH2 domain-binding affinity or the extended peptide nature of most inhibitors, which limits potency in whole cell systems where membrane transit is required.^{12,13} So, developing high-affinity Grb2-SH2 inhibitors that are specific, stable and cell-permeable is a formidable challenge.

Considering these affinity, bioavailability and specificity concerns, we developed a phage-display library-based screening strategy and discovered a disulfide-bridged cyclic decapeptide, termed **G1**, from 10⁷ different sequences.¹⁴ This nonphosphotyrosine-containing cyclopeptide specifically binds to the Grb2-SH2 domain, but does not bind to the homologous Src-SH2 domain. Based on this disulfide-cyclized peptide lead, a number of redox-stable thioether-cyclized analogues were developed (Figure 1), some of which exhibited potent binding affinity and encouraging levels of cellular activity.^{15–20} Apparently, the absence of a phosphate moiety in this family contributes to the remarkably high specificity and enhanced bioavailability, providing a new promising type of Grb2-SH2 domain binding motif that may advance the design of Grb2 antagonists.

To further improve the affinity and reduce the peptide character of the novel nonphosphorylated Grb2-SH2 domain

* To whom correspondence should be addressed. Phone: 86-21-50806876; Fax: +86-21-50806876; E-mail: yqlong@mail.shcnc.ac.cn.

[†] Shanghai Institute of Materia Medica.

[‡] SAIC-Frederick, Inc.

[§] National Cancer Institute.

^{||} University of Michigan.

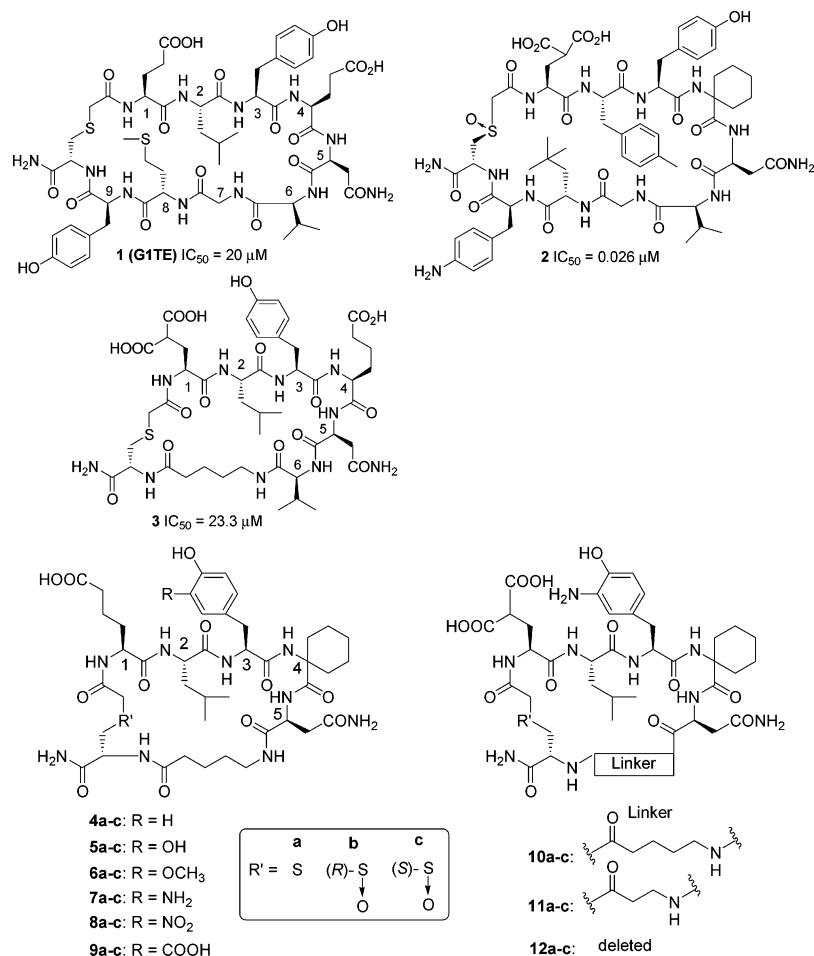


Figure 1. The structures of synthetic nonphosphorylated cyclopeptide ligands binding to the Grb2-SH2 domain.

inhibitor family, we were interested in developing a new scaffold with smaller ring size but higher affinity. Previous efforts to shorten the ring size resulted in a substantial loss of the inhibitory activity, but the introduction of an ω -amino carboxylic acid linker combined with favorable substitutions of Glu (γ -carboxyglutamic acid) for Glu¹ and Adi (amino adipic acid) for Glu⁴ resulted in a hexapeptide **3** (Figure 1) with an almost equal potency relative to G1TE.²⁰ Our previous SAR studies amply demonstrated that the carboxyl side chain of Glu¹ in G1TE partially compensates for the absence of the phosphate group on Tyr³, thus extending the side chain of Glu¹ by one CH₂ group ($X^1 = \text{Adi}$) or attaching one more carboxyl group to the side chain of Glu¹ ($X^1 = \text{Gla}$) greatly potentiated the binding of G1TE to the Grb2-SH2 domain.¹⁵ Considering the fact that the Grb2-SH2 domain preferentially binds to a protein or peptide ligand bearing a pY-X-N sequence in a β -turn conformation,²¹ we modified the hexapeptide protocol **3** by introducing a β -turn inducing amino acid, i.e., 1-aminocyclohexanecarboxylic acid (Ac6c), and deleting the sixth residue Val. The resulting pentapeptide platform **4** serves as a new template for further chemical elaboration.

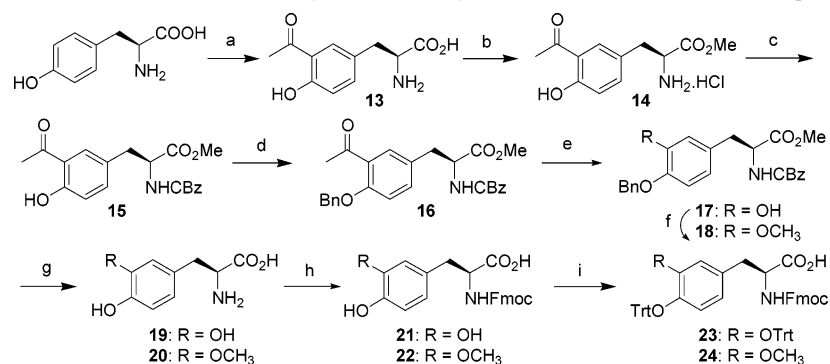
In the current paper, our effort was focused on the creation of novel tyrosine derivatives and their incorporation into the pentapeptide platform. We hypothesized that putting an electron-donating substituent such as an amino, methoxy or hydroxy group at the 3' position of Tyr, as a way of increasing the electronegativity of the aromatic ring and providing an additional hydrogen bonding moiety, would improve its interactions with arginine and serine residues in the binding site. As a comparison, an electron-withdrawing group such as nitro or carboxy was

introduced at the 3'-position of the tyrosine as well. This is a brand new strategy distinct from the conventional phosphotyrosine mimetic approach. As reported herein, the 3'-aminotyrosine-containing nonphosphorylated cyclic peptide **10b** (Figure 1) has been found to exhibit low-nanomolar Grb2-SH2 domain-binding potency ($IC_{50} = 58 \text{ nM}$) and antimetogenic effects against erbB-2-dependent breast cancers ($IC_{50} = 19 \text{ nM}$) with a sequence motif only 5 amino acids long (Glu¹-Leu-(3'-NH₂-Tyr)-Ac6c-Asn⁵), and without any phosphotyrosine or phosphotyrosine mimics. The SAR study, assisted by molecular modeling, led to new insights into the molecular recognition of the Grb2-SH2 domain by conformationally constrained nonphosphorylated peptide ligands.

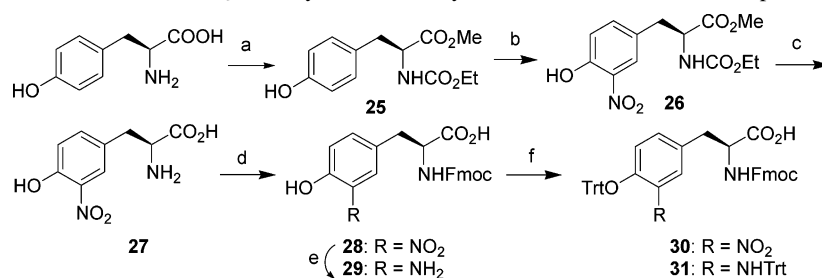
Synthesis

We designed a series of 3'-substituted tyrosine derivatives by introducing a nitro, amino, hydroxy, methoxy or carboxy group at the 3'-position of the phenol ring of tyrosine. Efficient approaches have been developed to synthesize the 3'-substituted tyrosine derivatives in protected forms bearing *N*- and *O*-trityl and *tert*-butyloxycarbonyl protections in the side chains and *N*- α -Fmoc protection at the backbone suitable for solid-phase peptide synthesis using the Fmoc protocol, as depicted in Schemes 1–3.

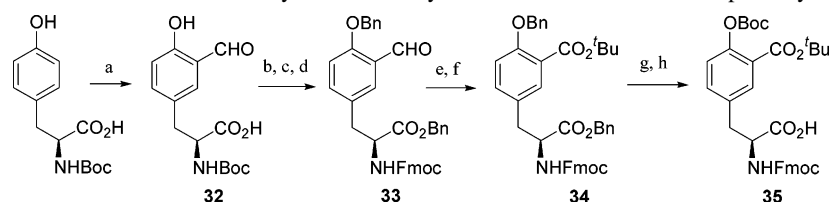
Tyrosine Derivatives L-3'-OH-Tyrosine (23) and L-3'-OCH₃-Tyrosine (24) in Globally Protected Form. As shown in Scheme 1, the preparation of orthogonally protected **23** and **24** started from commercially available L-tyrosine with initial Friedel-Crafts acylation followed by Fischer esterification and subsequent protection of the free amine and the free phenol as

Scheme 1. Synthetic Route toward the L-3'-OH/OCH₃-Tyrosine Suitably Protected for the Solid-Phase Peptide Synthesis

^a Reagents and conditions: (a) AlCl₃, CH₃COCl, PhNO₂, 100 °C; (b) SOCl₂, MeOH; (c) CbzCl, Na₂CO₃, Et₂O–H₂O (1:1); (d) BnBr, K₂CO₃, *n*-Bu₄NI, DMF; (e) (i) mCPBA, CH₂Cl₂; (ii) NH₃, MeOH; (f) CH₃I, K₂CO₃, DMF; (g) (i) H₂, 10% Pd–C; (ii) Na₂CO₃, H₂O–CH₃CN; (h) FmocOSu, 10% Na₂CO₃, H₂O/dioxane; (i) TrtCl, Et₃N, CH₃CN.

Scheme 2. Synthetic Route toward the L-3'-NO₂/NH₂-Tyrosine Suitably Protected for Solid -Phase Peptide Synthesis

^a Reagents and conditions: (a) (i) SOCl₂, MeOH; (ii) ClCO₂Et; (b) La(NO₃)₃, NaNO₃, HCl, CH₂Cl₂; (c) 10% KOH; (d) FmocOSu, 10% Na₂CO₃, H₂O/dioxane; (e) H₂, 10% Pd–C; (f) TrtCl, Et₃N, CH₃CN.

Scheme 3. Synthetic Route toward the L-3'-COOH-Tyrosine Suitably Protected for Solid-Phase Peptide Synthesis

^a Reagents and conditions: (a) 6 equiv NaOH, 2 equiv H₂O, CHCl₃, reflux; (b) 20% TFA in 10 mL CH₂Cl₂, rt; (c) 1.2 equiv FmocOSu, 10% Na₂CO₃, 0 °C to room temperature; (d) 1.5 equiv BnBr, 2.5 equiv K₂CO₃, *n*-Bu₄NI, DMF, rt; (e) 1.5 equiv Ag₂O, 1 equiv NaOH, rt; (f) 3 equiv *tert*-butyl 2,2,2-trichloroacetimidate, THF/hexane; (g) H₂, 10% Pd–C, EtOH, rt; (h) 2.0 equiv (Boc)₂O, cat. DMAP, 2.0 equiv Et₃N, DCM, rt.

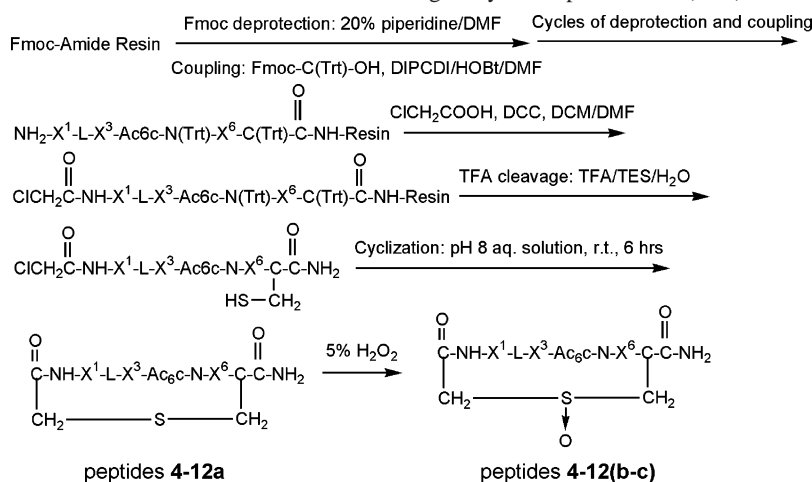
its carboxybenzyl ester and benzyl ether, respectively, providing the key intermediate **16**.²² Baeyer–Villiger oxidation and subsequent methanolysis of the resulting acetate by treatment with methanolic ammonia afforded *O*⁴-benzyl *N*-Cbz-L-DOPA methyl ester (**17**),²³ which was easily converted into *O*³-methyl-*O*⁴-benzyl *N*-Cbz-L-DOPA methyl ester (**18**). Catalytic hydrogenolysis of **17** and **18** followed by subsequent protection of the resulting free amine with Fmoc²⁴ and the free phenol with Trt group²⁵ afforded the final products **23** and **24** bearing global protections suitable for solid-phase peptide synthesis based on Fmoc chemistry.

Tyrosine Derivatives L-3'-NO₂-Tyrosine (30) and L-3'-NH₂-Tyrosine (31) in Orthogonally Protected Form. Starting from commercially available L-Tyr-OH, as outlined in Scheme 2, we prepared **25** in quantitative yield by esterification of the α -carboxy acid with thionyl chloride in methanol followed by protection of the amino group with ethyl chloroformate in an aqueous NaHCO₃ solution. Selective nitration at the 3'-position of **25** was accomplished in 85% yield by using La(NO₃)₃ as a homogeneous catalyst and NaNO₃/HCl as the nitration reagent.²⁶ Treatment of **26** with 10% potassium hydroxide followed by reprotection with Fmoc-OSu provided *N*- α -Fmoc-3'-nitro-tyrosine **28**, which was readily converted into the corresponding

3'-aminotyrosine **29** by the catalytic hydrogenation. The subsequent protection of the amino group and hydroxy group by trityl chloride²⁵ afforded the 3'-nitrotyrosine **30** and 3'-aminotyrosine **31** in orthogonal protections suitable for solid-phase peptide synthesis.

Tyrosine Derivative L-3'-COOH-Tyrosine in Globally Protected Form (35). The introduction of a carboxyl group at the 3'-position of the L-tyrosine was accomplished by using Reimer–Tiemann reaction as a key step.²⁷ As outlined in Scheme 3, treatment of the *N*-Boc-L-tyrosine with chloroform and solid sodium hydroxide in the presence of a small amount of water gave the desired 3-formyl compound **32**.²⁷ Transformation of the *N*-Boc protection into *N*-Fmoc followed by the benzylation of the phenol and the α -carboxyl acid provided compound **33**. Oxidation of the formyl group of **33** with Ag₂O under basic condition and subsequent esterification of the resulting carboxylic acid with *tert*-butyl 2,2,2-trichloroacetimidate provided the fully protected compound **34**. Hydrogenation removes the benzyl protecting groups, and the treatment with (Boc)₂O gave the desired product **35** orthogonally protected for solid-phase peptide synthesis.

Cyclopeptide Synthesis. The simplified pentapeptide platform **4a** served as the template for the incorporation of the 3'-

Scheme 4. General Synthetic Route for Thioether- and Sulfoxide-Bridged Cyclic Peptides **4–12(a–c)**

substituted tyrosine derivatives with global protections. The synthesis of thioether- or sulfoxide-bridged cyclic peptides **4–12(a–c)** was carried out in a manner similar to that reported previously (Scheme 4).²⁰

Molecular Modeling. The interactions of peptides **4a–9a** with the Grb2 SH2 domain protein were examined using molecular modeling techniques. Structures for the peptides were built by modifying the X-ray crystal structure of the KPF-pYVNV peptide bound to the Grb2-SH2 domain.²¹ The tyrosine ring can adopt two symmetrical orientations, one with the 3' substituent facing up, toward the rest of the peptide, and one with the 3' substituent facing down into the binding site (Figure 2).

Both orientations of the tyrosine ring were modeled, since it was not possible to know a priori which one is lower in energy for each peptide. Molecular dynamics was used to allow the peptide to relax into the binding site while exploring available conformational space, and snapshots from the trajectory were saved periodically. The lowest energy structure for each system was further analyzed to calculate the interaction energy between the peptide and the receptor. This gives an estimate of the enthalpic portion of the binding energy.

Results and Discussion

The objective of the current work was to examine the Grb2-SH2 domain binding effects incurred by (1) the substitution at

the 3'-position of the phenol ring of the tyrosine residue within the consensus sequence of a nonphosphorylated cyclic peptide ligand, and (2) shortening or deleting the ω -amino acid linker. Various substituents displaying different electronic effects were incorporated into the 3'-position of the phenol ring of the key tyrosine residue. A simplified pentapeptide platform bearing the 5 amino acid long sequence of Adi-L-Y'-Ac6c-N served as the starting point to determine the optimal 3'-substitution (**4–9(a–c)**). In combination with the favorable substitution of Glu in position 1, we investigated the effect of the length of the ω -amino acid linker on Grb2 SH2 domain binding potency within the pentapeptide scaffold of Glu¹-L-(3'-NH₂Tyr)-Ac6c-N⁵ (**10–12(a–c)**).

3'-Aminotyrosine Significantly Enhances the Grb2-SH2 Binding. Since reducing peptidic character is an important issue in the development of Grb2-SH2 domain antagonists as chemotherapeutic agents, we developed a new small peptide platform with the minimum active sequence of E¹-Xx-Y-Xx⁴-N⁵, having a β -turn inducing amino acid (i.e. Ac6c) in position 4 and a favorable substitution of Adi for Glu in position 1.¹⁵ The resulting pentapeptide **4a** displayed moderate Grb2-SH2 domain binding (**4a**, IC₅₀ = 93 μ M) with minimum negative charge. Consistent with previous findings, when the thioether-cyclized peptide **4a** was oxidized into the relatively more rigid *R*-configured sulfoxide **4b**, the binding affinity was slightly improved (**4b**, IC₅₀ = 77 μ M). However, the *S*-configured

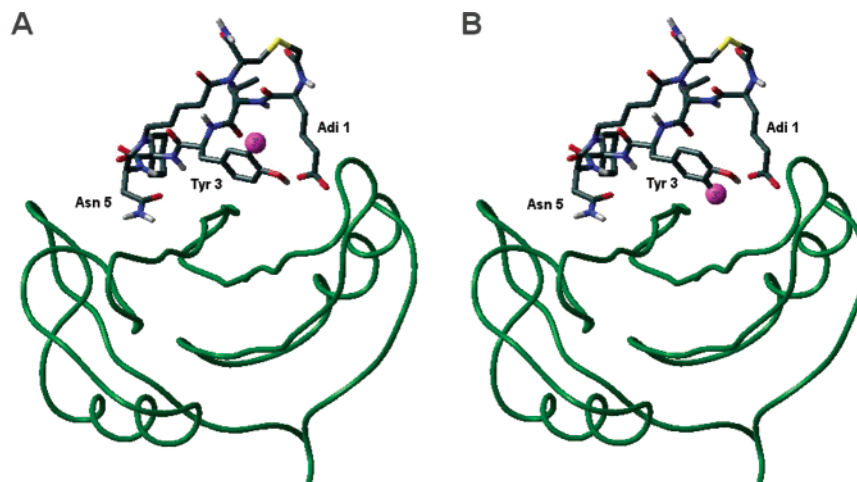


Figure 2. Two possible orientations of the 3'-substituted tyrosine ring relative to the Grb2-SH2 domain binding site. The protein backbone is shown as a green ribbon, and the location of the 3' substituent is shown with a magenta ball. A: "up" orientation of the 3' substituent. B: "down" orientation of the 3' substituent.

Table 1. Grb2-SH2 Domain Inhibitory Activity of the Peptides 4–9(a–c) with the General Structure Cyclo-(CH₂CO-Adi¹-Leu²-X³-Ac6c⁴-Asn⁵-Ava⁶-X⁷)-amide^a

compd	modifications of amino acid residues		IC ₅₀ (μM) ^b
	X ³	X ⁷	
4a	Tyr	Cys	93 ± 13
5a	3-OH-Tyr	Cys	135 ± 35
6a	3-OCH ₃ -Tyr	Cys	245 ± 35
7a	3-NH ₂ -Tyr	Cys	8.9 ± 4.0
8a	3-NO ₂ -Tyr	Cys	182 ± 32
9a	3-COOH-Tyr	Cys	88 ± 5
4b	Tyr	Cys(O)-(R)	77 ± 13
5b	3-OH-Tyr	Cys(O)-(R)	87 ± 8
6b	3-OCH ₃ -Tyr	Cys(O)-(R)	97 ± 2
7b	3-NH ₂ -Tyr	Cys(O)-(R)	3.9 ± 0.2
8b	3-NO ₂ -Tyr	Cys(O)-(R)	25 ± 3
9b	3-COOH-Tyr	Cys(O)-(R)	16 ± 4
4c	Tyr	Cys(O)-(S)	1000
5c	3-OH-Tyr	Cys(O)-(S)	550 ± 70
6c	3-OCH ₃ -Tyr	Cys(O)-(S)	> 1000
7c	3-NH ₂ -Tyr	Cys(O)-(S)	14 ± 2
8c	3-NO ₂ -Tyr	Cys(O)-(S)	265
9c	3-COOH-Tyr	Cys(O)-(S)	212 ± 28

^a The binding assay was performed on a BIAcore 3000 instrument by the method described in the Experimental Section. ^b Values are the mean of at least two independent experiments and are expressed as the concentration at which half-maximal competition was observed (IC₅₀). Standard deviation is given in parentheses.

sulfoxide **4c** was much less active (**4c**, IC₅₀ = 1000 μM) than its precursor thioether analogue **4a**, probably due to a change in the peptide backbone conformation caused by the repulsion of the sulfoxide functional group with the carbonyl group of the C-terminal Cys, as was observed in G1TE analogues with a nine-amino acid long sequence.¹⁷ Starting from the pentapeptide platform **4**, a series of tyrosine derivatives bearing various substituents at the 3'-position of the phenol ring were incorporated as the surrogate of tyrosine in the position 3.

As shown in Table 1, the electronic and structural effects of the 3'-substituent of tyrosine did play an important role in the interaction of the nonphosphorylated cyclic peptide ligand with the Grb2-SH2 protein. As expected, an electron-donating group such as the amino substituent improved the binding interactions significantly, resulting in a 10-fold enhancement in potency (**7a**, IC₅₀ = 8.9 μM) relative to the parent peptide **4a**. The corresponding (*R*)-sulfoxide cyclized analogue is more active (**7b**, IC₅₀ = 3.9 μM) and the (*S*)-sulfoxide cyclized analogue is much less active (**7c**, IC₅₀ = 14 μM). However, both the hydroxy and methoxy group are less advantageous for Grb2-SH2 binding (**5a**, IC₅₀ = 135 μM; **6a**, IC₅₀ = 245 μM) even though these are electron-donating groups as well. Accordingly, the (*R*)-sulfoxide-cyclized analogues displayed an improved activity (**5b**, IC₅₀ = 87 μM; **6b**, IC₅₀ = 97 μM) and the (*S*)-sulfoxide-cyclized analogues suffered a marked drop in the potency (**5c**, IC₅₀ = 550 μM; **6c**, IC₅₀ > 1000 μM).

In comparison, an electron-withdrawing group at the 3'-position of the tyrosine is detrimental to the Grb2-SH2 binding in terms of electronic effects. This is exemplified by the 3'-nitro functionality. The 3'-nitrotyrosine-containing pentapeptide **8a** (IC₅₀ = 182 μM) is 2-fold less potent than the parent peptide **4a**. Further modification was undertaken on the cyclization linkage, and the same results were observed: the (*R*)-sulfoxide cyclized analogue is much more potent (**8b**, IC₅₀ = 25 μM) and the (*S*)-sulfoxide cyclized one is less active (**8c**, IC₅₀ = 265 μM). Interestingly, another electron-withdrawing group such as carboxyl functionality can maintain the binding potency when introduced in the 3'-position of the tyrosine (**9a**, IC₅₀ = 88 μM), and the oxidation of the thioether linkage of **9a** resulted in a

Table 2. Interaction Energies of Peptides 4a–9a with the Grb2-SH2 Domain Calculated by Molecular Modeling, Compared to the Experimental IC₅₀ Values^a

peptide	total energy (kcal/mol)	IC ₅₀ (μM)
4a: Tyr	-309.16	93
5a: 3'-OH-Tyr "up"	-294.93	135
5a: 3'-OH-Tyr "down"	-285.97	
6a: 3'-OCH ₃ -Tyr "up"	-278.95	245
6a: 3'-OCH ₃ -Tyr "down"	-301.76	
7a: 3'-NH ₂ -Tyr "up"	-329.38	8.9
7a: 3'-NH ₂ -Tyr "down"	-298.87	
8a: 3'-NO ₂ -Tyr "up"	-255.39	182
8a: 3'-NO ₂ -Tyr "down"	-245.61	
9a: 3'-COOH-Tyr "up"	-283.66	88
9a: 3'-COOH-Tyr "down"	-328.64	

^a The energy value for the lowest-energy conformation of each peptide is marked in bold.

dramatic increase in the affinity of the (*R*)-configured analogue (**9b**, IC₅₀ = 16 μM), whereas the diastereoisomeric (*S*)-sulfoxide cyclized analogue still displayed decreased activity (**9c**, IC₅₀ = 212 μM). The inconsistency of the electronic effect of the 3'-substitution at the tyrosine on the overall binding to the Grb2-SH2 protein might be attributed to the additional contribution of the structural effect of the substituent at the 3'-position. These observations can be rationalized by the molecular modeling results.

Molecular Modeling of the Structural and Energetic Effects of 3' Tyrosine Substitution. The calculated interaction energies for each peptide in complex with the Grb2-SH2 domain are summarized in Table 2 below.

For the 3'-OH-Tyr, 3'-NH₂-Tyr, and 3'-NO₂-Tyr peptides, the "up" orientation, with the substituents on the tyrosine ring facing up toward the rest of the peptide, is lower in energy. Somewhat counterintuitively, for the bulkier 3'-OCH₃-Tyr and 3'-COOH-Tyr peptides, the "down" orientation, with the substituents on the tyrosine ring facing down into the binding site, is more favorable. This is because in the "up" orientation the bulkier substituents bump against the linker region of the peptide, altering its backbone conformation. The total interaction energies of the lowest-energy conformation for each peptide qualitatively follow the trend in IC₅₀ values, with 3'-NH₂-Tyr and 3'-COOH-Tyr having stronger interactions than unsubstituted Tyr, 3'-OH-Tyr and 3'-OCH₃-Tyr being slightly weaker, and 3'-NO₂-Tyr significantly weaker.

The modeled structures of the peptides bound to the Grb2-SH2 domain (Figure 3) can help explain both the experimentally observed differences in binding affinity and the modeled interaction energy values. The binding modes of all the peptides are similar to previously studied G1TE peptides. The Tyr³ and Adi¹ residues replace the phosphate group of the natural ligand by forming a network of hydrogen bonds to Grb2-SH2 domain residues Arg67, Arg86, Ser88, Ser90, and Ser96, with an additional cation-π interaction between the phenol ring of Tyr³ and the guanidinium group of Arg67 (Figure 3A). The structural effects of adding an electron-donating or electron-withdrawing group to the tyrosine ring vary depending on the size and hydrogen-bonding ability of the substituent.

In the case of the electron-donating substituents, the hydroxy group in peptide **5a** (Figure 3B) forms an additional hydrogen bond with Lys109, but this changes the orientation of the ring in the binding site, pulling it away from Arg67 and disrupting the cation-π interaction. The bulkiness of the methoxy group in peptide **6a** (Figure 3C) forces the tyrosine ring to sit higher in the binding site, breaking the hydrogen bond to Ser96 and

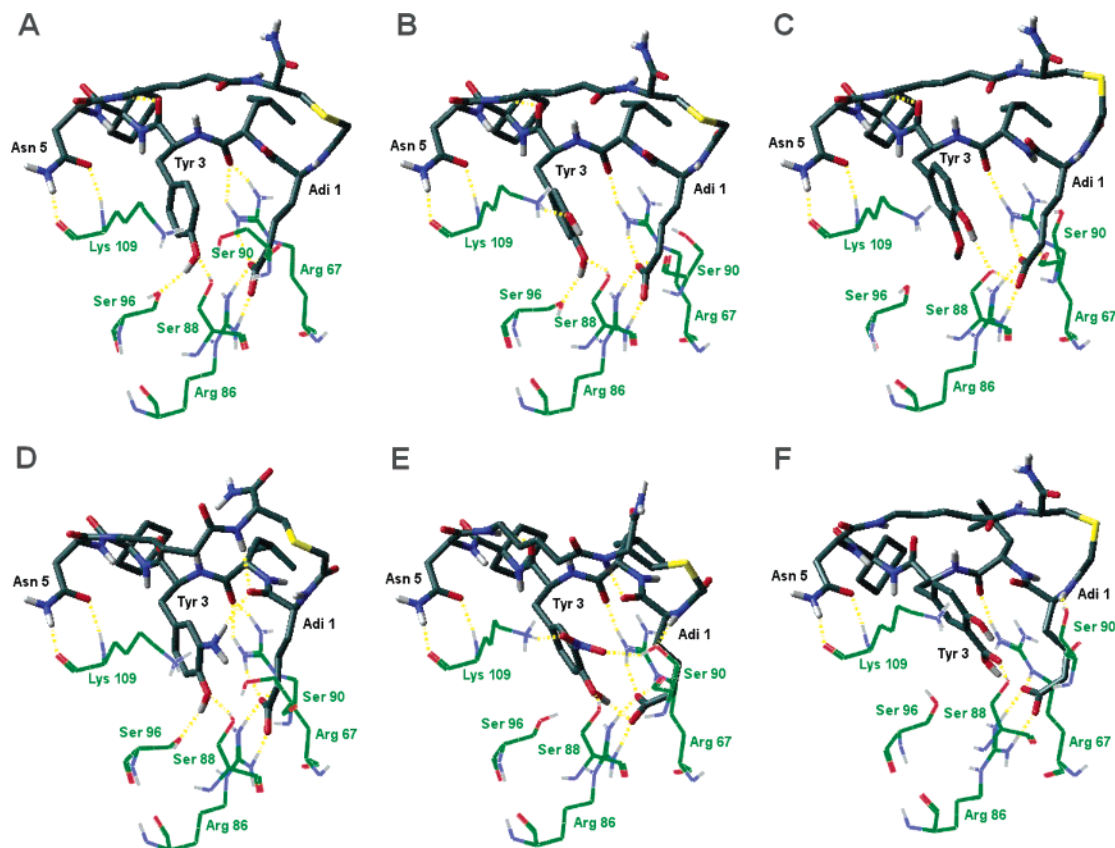


Figure 3. The calculated binding modes of peptides **4a–9a** with the Grb2-SH2 protein. The peptide is drawn with thick lines, and with carbon atoms colored dark gray. The receptor residues are drawn with thinner lines, and with carbon atoms colored green. A: peptide **4a** containing Tyr. B: peptide **5a** containing 3'-OH-Tyr. C: peptide **6a** containing 3'-OCH₃-Tyr. D: peptide **7a** containing 3'-NH₂-Tyr. E: peptide **8a** containing 3'-NO₂-Tyr. F: peptide **9a** containing 3'-COOH-Tyr.

weakening all of the peptide-receptor interactions. However, the amino group in peptide **7a** (Figure 3D) can also form an additional hydrogen bond with the backbone carbonyl of Adi¹, which in turn hydrogen bonds to the backbone nitrogen of Cys⁷, stabilizing the bound conformation of the peptide. The aromatic ring does not shift its position, and the cation- π interaction with Arg67 is strengthened.

In the case of the electron-withdrawing substituents, the nitro group in peptide **8a** (Figure 3E) forms a salt bridge with Lys109 and a strong hydrogen bond to Ser90. As with the hydroxy substituent in peptide **5a**, this changes the orientation of the ring in the binding site as well as the shape of the binding site itself, such that the Adi¹ residue must adopt a strained conformation. With the carboxy group in peptide **9a** (Figure 3F), as with the methoxy substituent in peptide **6a**, the tyrosine ring sits higher in the binding site, but the overall interaction between the peptide and the receptor is not weakened because the carboxy group makes extensive hydrogen bonding interactions with Ser88 and Arg67.

The electronic effects of the ring substituents at the 3' position of Tyr³ on the strength of the cation- π interaction between the phenol ring and Arg67 are relatively weak compared to the hydrogen bonding or salt bridge interactions that the substituents can form with other residues in the binding site. In all cases except for the amino substituent in peptide **7a**, these additional interactions are strong enough to alter the orientation of the Tyr³ residue in the binding site and disrupt the interaction of the aromatic ring with the guanidinium group of Arg67.

Combination of Optimal Structural Features and the Modification of the ω -Amino Acid Linker Length. We have previously found that the Glu¹ side chain in GITE (**1**)

compensates for the absence of Tyr³ phosphorylation in retaining effective binding to the Grb2-SH2 domain.¹⁵ Replacement of Glu¹ with Adi or Gla prominently improves binding affinity, and Gla is more favored than Adi.^{15–20} As suggested by molecular modeling,^{15,16} the side chains of Gla¹ and Tyr³ both point in the same direction within the partially vacant pTyr-binding pocket and form an intramolecular hydrogen bond between the hydroxyl group of Tyr³ and one of the carboxyl groups of Gla¹. On the basis of these findings, we developed a fully elaborated cyclic pentapeptide **10a** with Gla in position 1 and 3'-aminotyrosine in position 3. The introduction of an electron-donating amino group at the 3' position of Tyr, to provide an electron-rich aromatic ring and an additional hydrogen-bond donor, resulted in a significant enhancement of the Grb2-SH2 domain binding affinity (**10a**, IC₅₀ = 0.19 μ M). As expected, when the thioether linkage of **10a** was oxidized into the *R*-configured sulfoxide to give inhibitor **10b**, the binding affinity was remarkably improved with an IC₅₀ = 58 nM, which is 3.3-fold more potent than **10a** and 1608-fold more potent than the parent peptide **4a**. Also as expected, the *S*-configured sulfoxide analogue **10c** (IC₅₀ = 1.55 μ M) was 8.1 times less potent than its thioether counterpart. Notably, compound **10b** is one of the most potent and smallest nonphosphorus-containing Grb2-SH2 domain antagonists reported to date.

Comparing the binding affinity of **10b** and a recently reported cyclic hexapeptide analogue with a binding motif sequence of Gla-Leu-(3'-NH₂-Tyr)-Ac6c-Asn-Val,²⁸ a small difference was observed between their inhibitory activities. So we hypothesize that the insertion of a β -turn inducing amino acid, i.e., Ac6c, helps to improve the local and global conformational constraint; thus the linker might be reduced or deleted. As shown in Table

Table 3. Grb2-SH2 Domain Inhibitory Activity of the Peptides **10–12**(a–c) with the General Structure Cyclo-(CH₂CO-Gla¹-Leu²-(3-NH₂-Tyr)³-Ac6c⁴-Asn⁵-X⁶-X⁷)-amide^a

compd	modifications of amino acid residues		IC ₅₀ (μM) ^b
	X ⁶	X ⁷	
10a	Ava	Cys	0.19 ± 0.03
11a	β-Ala	Cys	1.02 ± 0.20
12a	deleted	Cys	22.5 ± 0.5
10b	Ava	Cys(O)-(R)	0.058 ± 0.007
11b	β-Ala	Cys(O)-(R)	0.36 ± 0.08
12b	deleted	Cys(O)-(R)	9.7 ± 4.2
10c	Ava	Cys(O)-(S)	1.55 ± 0.25
11c	β-Ala	Cys(O)-(S)	11.2 ± 0.3
12c	deleted	Cys(O)-(S)	200 ± 60

^a The binding assay was performed on a BIAcore 3000 instrument by the method described in the Experimental Section. ^b Values are the mean of at least two independent experiments and are expressed as the concentration at which half-maximal competition was observed (IC₅₀). Standard deviation is given in parentheses.

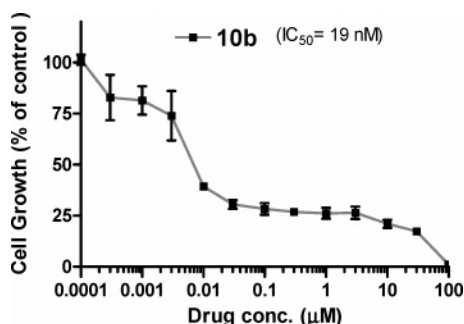


Figure 4. Inhibition of cell growth by a potent Grb2 SH2 inhibitor (compound **10b**) in MDA-MB-435 breast cancer cells as determined using a WST-based assay.

3, the shortening of the linker length by two methylene units resulted in an acceptable loss of the binding affinity by 5.4-fold (**11a**, IC₅₀ = 1.02 μM); however, the deletion of the ω-amino valeric acid linker caused a 118-fold decrease in the binding potency (**12a**, IC₅₀ = 22.5 μM). The oxidation of the thioether linkage into sulfoxide restored the binding affinity, affording the higher-affinity (R)-configured analogues (**11b**, IC₅₀ = 0.36 μM; **12b**, IC₅₀ = 9.7 μM) and the lower-affinity (S)-configured analogues (**11c**, IC₅₀ = 11.2 μM; **12c**, IC₅₀ = 200 μM). These newly designed and simplified nonphosphorylated cyclic ligands of the Grb-SH2 domain provide new templates for further chemical elaboration to improve the activity.

Antiproliferative Effects in Breast Cancer Cells in Culture. SPR-derived IC₅₀ values provide an indication of the ability of synthetic agents to bind to isolated Grb2-SH2 protein in an extracellular setting. Such measurements do not reflect the situation in whole cells, where inhibitors must cross cell membranes prior to interacting with protein targets. Therefore, cell proliferation assays were conducted to evaluate the effectiveness of our synthetic peptides to inhibit the intracellular association of native Grb2 protein with activated cellular growth factor receptor. MDA-MB-453 breast cancer cell line was used, which overexpresses erbB-2,²⁹ mitogenically driven through Grb2-dependent signaling pathways. The best Grb2-SH2 inhibitor **10b** was selected for this purpose. Very encouragingly, treatment of MDA-MB-453 cancer cells with **10b** provides potent antimetabolic effects with an IC₅₀ value of 19 nM (Figure 4), which represents the highest cellular activity yet reported for a synthetic Grb2-SH2 domain inhibitor free of phosphotyrosine or phosphotyrosine mimics. As a comparison, little antimetabolic effect was observed in A-431 epidermoid cancer cells, which overexpress EGFR and lack erbB-2 growth

dependence, even at the concentration of 100 μM of the inhibitor **10b**. These results indicate that **10b** is able to penetrate the cell membrane and effectively block erbB-2-driven growth in breast cancer cells at low nanomolar concentrations that are not cytotoxic to cells not dependent on this signaling pathway.

Conclusions

In this study, we designed a series of tyrosine derivatives bearing various substituents at the 3'-position, developed new approaches to synthesize L-3'-substituted tyrosines suitably protected for solid-phase peptide synthesis and successfully incorporated them into a new structural motif binding to the Grb2 SH2 domain with a sequence only five amino acids long. The 3'-aminotyrosine-containing sulfoxide-cyclized pentapeptide (**10b**) exhibited potent Grb2-SH2 domain binding affinity with an IC₅₀ = 58 nM and excellent antiproliferative activity against erbB-2-dependent MDA-MB-453 breast cancer cells with an IC₅₀ = 19 nM, which represents the highest cellular activity yet reported for a synthetic Grb2 SH2 domain inhibitor free of phosphotyrosine or phosphotyrosine mimics. The interaction between the 3'-amino group of Tyr³ and the backbone of the cyclic peptide stabilizes a favorable conformation for the peptide binding to the Grb2-SH2 domain; furthermore, the electron-donating ability of the amino group at the 3' position of Tyr seems to contribute to a strengthened interaction between the electron-rich phenol ring and the Arg67 side chain of the Grb2 SH2 domain binding cavity. This fully elaborated small peptidomimetic **10b** with low-nanomolar cellular activity and reduced peptidic nature provides a novel template for the development of non-pTyr-containing Grb2-SH2 domain antagonists and potentially may find value in chemical therapeutics for erbB2-related cancers. More significantly, the utilization of 3'-substituted tyrosine provides a new solution to the tradeoff between the need for negatively charged pTyr mimetics for optimal affinity and the need to minimize charge to facilitate cell entry for all SH2 domain inhibitors.

Experimental Section

Binding Affinity Measurements Using Surface Plasmon Resonance (SPR) Analysis. The competitive binding affinity of ligands for the Grb2-SH2 protein was assessed using Biacore SPR methods on a BIAcore 3000 instrument (Pharmacia Biosensor, Uppsala, Sweden). IC₅₀ values were determined by mixing the inhibitor with recombinant Grb2 SH2 protein and measuring the amount of binding at equilibrium to an immobilized SHC (pTyr-317) phosphopeptide, i.e., biotinyl-DDPS-pY-VNVQ, in a manner similar to that reported previously.¹⁴

Examination of Antiproliferative Effects of Synthetic Antagonists against Breast Cancer Cells in Culture. MDA-MB-453 cells were seeded in 96-well flat bottom cell culture plates at a density of (3–4) × 10³ cells/well with compounds and incubated for 4 days. Cell growth inhibition after treatment with the various concentrations of the compounds was determined by WST-8 (2-(2-methoxy-4-nitrophenyl)-3-(4-nitrophenyl)-5-(2,4-disulfophenyl)-2H-tetrazolium monosodium salt (Dojindo Molecular Technologies Inc., Gaithersburg, MD). WST-8 was added at a final concentration of 10% to each well, and then the plates were incubated at 37 °C for 2–3 h. The absorbance of the samples was measured at 450 nm using a TECAN ULTRA Reader. Concentration of the compounds that inhibited cell growth by 50% (IC₅₀) was calculated by comparing absorbance in the untreated cells (DMSO control), and the cells treated with the varying concentrations of compounds.

Molecular Modeling. The peptide models were built from PDB structure 1TZE²¹ in the following way. First, the residues Lys¹, Pro², and Val⁷ were deleted, Phe³ was mutated to Leu, the phosphate group on Tyr⁴ was removed, and Val⁵ was mutated to Ac6c. Then

the Ava and amidated Cys linking residues were added to the C-terminal end and the acylated Adi residue was built into the N-terminal end. The N- and C-terminal ends were linked, and the backbone was energy minimized. The 3' substituents were added to the Tyr⁴ ring in both possible orientations.

Simulations were performed with MacroModel 9.0,³⁰ using the OPLS2003 force field.³¹ All runs were done at 300 K with a time step of 1.0 fs, using implicit water solvent, with a constant dielectric of 1.0 and extended cutoffs of 8.0 Å for van der Waals interactions, 20.0 Å for electrostatic interactions, and 4.0 Å for hydrogen bonding interactions. The SHAKE procedure³² was used to constrain bonds to hydrogen atoms. Residues in the Grb2 SH2 domain within 5 Å of the binding site were free to move, but the rest of the receptor was fixed in place. The peptide residue Asn⁵ was tethered to its pocket in the binding site by constraining the three hydrogen bonds it forms with the receptor to a distance of 2.0 + 0.5 Å with a force constant of 100 kcal/mol.

Each peptide–receptor system first underwent 100 steps of PRCG minimization and then was equilibrated with 10 ps of molecular dynamics. This was followed by a production run of 500 ps of molecular dynamics, with the coordinates of the system saved every 1 ps. Each of these saved structures was minimized to convergence with a maximum gradient of 0.05. The lowest-energy structure for each system was further analyzed with an eMBrAcE energy difference calculation, which estimates the energy changes upon association of a ligand with a receptor.

General Synthesis. ¹H NMR spectra were recorded on a Varian Mercury-400 MHz spectrometer. The data are reported in parts per million relative to TMS and referenced to the solvent in which they were run. Elemental analyses were obtained using Vario EL spectrometer. Melting points (uncorrected) were determined on a Buchi-510 capillary apparatus. EI-MS spectra were obtained on a Finnigan MAT 95 mass spectrometer, and ESI-MS spectra were recorded on a Finnigan LCQ Deca mass spectrometer. Specific rotations (uncorrected) were determined in a Perkin-Elmer 341 polarimeter. The solvent was removed by rotary evaporation under reduced pressure, and flash column chromatography was performed on silica gel H (10–40 μm). Anhydrous solvents were obtained by redistillation over sodium wire.

All peptides were synthesized manually using standard solid-phase peptide chemistry with Fmoc protected amino acids on Pal resin at a 0.1 mmol scale. Couplings with Fmoc amino acids (2.5 equiv) were performed in the presence of 1-hydroxybenzotriazole (HOBT) and 1,3-diisopropylcarbodiimide (DIPCDI) (each 2.5 equiv) in DMF (5 mL) at room temperature for 2 h, and then the Fmoc protecting group was removed by treatment with 20% piperidine in DMF (5 mL) at room temperature for 20 min. The synthesis of the thioether- and sulfoxide-bridged cyclic peptides were similar to the procedure described previously.^{18,20} The final product was purified by semipreparative reverse phase HPLC. RP-HPLC conditions: Vydac C18 column (20 × 250 mm); solvent gradient system 1, A, 0.05% TFA in water; B, 0.05% TFA in 90% acetonitrile in water; solvent gradient system 2, A, 0.05% TFA in water; C, 0.05% TFA in 90% methanol in water with gradient indicated below; flow rate, 2.5 mL/min, UV detector, 225 nm. ESI-MS was performed on a Finnigan LCQ Deca mass spectrometer. The purity of products was characterized by analytical HPLC and ESI-MS. HPLC using two solvent systems: method 1, gradient 10–70% B over 30 min; method 2, gradient 10–70% C over 30 min.

L-3-(3-Acetyl-4-hydroxyphenyl)alanine Hydrochloride (13).²² Anhydrous aluminum chloride (26.7 g, 0.2 mol) was added to a solution of L-tyrosine (10 g, 0.05 mol) in 200 mL of dry nitrobenzene at 25 °C. The reaction mixture was stirred at 25 °C until homogeneous. Acetyl chloride (4.71 g, 0.06 mol) was added in one portion and was accompanied by an immediate color change from red to yellow. The reaction mixture was warmed at 100 °C with stirring for 6 h, then cooled to room temperature and was poured over a mixture of 300 g of ice and 50 mL of concentrated HCl. The nitrobenzene layer was separated and the aqueous phase was washed with ethyl acetate. The aqueous mixture was concen-

trated in vacuo to ca. a 100 mL volume, and the concentrated solution was allowed to stand at 0 °C for 12 h. The precipitated solid was collected by filtration and recrystallized (5 N HCl) to afford **13** (10 g, yield 67%) as yellow needles. Mp 218–222 °C (lit.²² mp 220–224 °C).

L-3-(3-Acetyl-4-hydroxyphenyl)alanine Methyl Ester Hydrochloride (14).²² To solution of **13** (4.3 g, 23 mmol) in 50 mL of methanol was added thionyl chloride (6 mL, 0.084 mol) in a dropwise manner at –10 °C. After the addition the solution was allowed warm to room temperature. The reaction mixture was heated at reflux overnight and then concentrated via rotary evaporator to afford the crude ester. Recrystallization from MeOH–CH₂Cl₂ (1:4) afforded **14** (8.5 g, yield 74%) as yellow needles. Mp 179–183 °C (lit.²² mp 180–183 °C).

L-3-(3-Acetyl-4-hydroxyphenyl)-N-(benzyloxycarbonyl)alanine Methyl Ester (15). Amine hydrochloride **14** (2.23 g, 10.0 mmol) in a two-phase mixture of 50 mL of water and 40 mL of Et₂O at 25 °C was treated with sodium carbonate (3.20 g, 30.0 mmol, 3.0 equiv) and benzyl chloroformate (1.5 mL, 10 mmol, 1.0 equiv), and the resulting mixture was stirred for 3 h at 25 °C. The ether layer was separated, washed with saturated aqueous NaCl, dried over MgSO₄, and concentrated in vacuo to afford yellow oil. Chromatography with Et₂O afforded **15** (4.0 g, yield 93%) as a clear viscous oil which was solidified on standing. Mp 95 °C (lit.²² mp 94–96 °C); ¹H NMR (CDCl₃, 400 MHz) δ ppm 7.42 (s, 1H), 7.30 (m, 5H), 7.17 (d, 1H, *J* = 9.2 Hz), 6.85 (d, 1H, *J* = 8.8 Hz), 5.25 (br d, 1H, *J* = 8.4 Hz), 5.11 (d, 1H, *J* = 12.0 Hz), 5.02 (d, 1H, *J* = 12.0 Hz), 4.70–4.66 (m, 1H), 3.69 (s, 3H), 3.13–3.06 (m, 2H), 2.51 (s, 3H).

L-3-(3-Acetyl-4-(benzyloxy)phenyl)-N-(benzyloxycarbonyl)alanine Methyl Ester (16).²² A solution of the phenol **15** (0.9 g, 2.41 mmol) in dry DMF (10 mL) at room temperature was treated with benzyl bromide (0.29 mL, 2.41 mmol, 1.0 equiv), potassium carbonate (0.67 g, 4.83 mmol, 2.0 equiv), and tetra-*n*-butylammonium iodide (89 mg, 0.24 mmol, 0.1 equiv), and the resulting reaction mixture was stirred at room temperature (6 h). The reaction mixture was filtered and the filtrate was poured into 10 mL of water and was extracted with EtOAc (usual workup). Flash chromatography (EtOAc/PE = 3/10 as eluant) afforded **16** (0.64 g, 60%) as a colorless oil which solidified on standing to give a white solid. Mp 86–89 °C (lit.²² mp 87–90 °C); ¹H NMR (CDCl₃, 400 MHz) δ ppm 7.50 (d, 1H *J* = 2.4 Hz), 7.40–7.32 (m, 10H), 7.17 (dd, 1H, ¹*J* = 8.4 Hz, ²*J* = 2.4 Hz), 6.91 (d, 1H, *J* = 8.4 Hz), 5.22 (br d, 1H, *J* = 8.4 Hz), 5.12–5.09 (m, 4H), 4.72–4.60 (m, 1H), 3.74 (s, 3H), 3.13–3.06 (m, 2H), 2.54 (s, 3H).

L-3-(3-Hydroxy-4-(benzyloxy)phenyl)-N-(benzyloxycarbonyl)alanine Methyl Ester (17).²³ A solution of **16** (686 mg, 1.49 mmol) in 10 mL of dry CH₂Cl₂ was treated with mCPBA (57–85%, 738 mg) and warmed at 40 °C overnight. The solution was diluted with ether and washed with saturated sodium thiosulfate, saturated sodium bicarbonate, and brine, dried over sodium bicarbonate, filtered, and concentrated in vacuo. The residue was dissolved in 10 mL of CH₂Cl₂ and a 2 M solution of ammonia in methanol 1 mL was added, and the mixture was stirred for 1 h and concentrated. The residue was treated by usual workup. The crude product was purified on silica gel with 1:2 ethyl acetate–PE to give **17** as a colorless syrup (453 mg, yield 70%). ¹H NMR (CDCl₃, 400 MHz): δ ppm 7.42 (s, 5H), 7.34–7.28 (m, 5H), 6.78 (d, 1H, *J* = 8.4 Hz), 6.58 (dd, 1H, *J* = 8.4 Hz, *J* = 2.4 Hz), 6.46 (d, 1H, *J* = 2.4 Hz), 5.28 (br d, 1H, *J* = 8.4 Hz), 5.04–4.99 (m, 2H), 4.61–4.53 (m, 1H), 3.69 (s, 3H), 3.14–2.95 (m, 2H).

L-3-(3-Methoxy-4-(benzyloxy)phenyl)-N-(benzyloxycarbonyl)alanine Methyl Ester (18).²³ A solution of **17** (513 mg, 1.18 mmol) in dry DMF (20 mL) was treated with CH₃I (2 mL, 3.54 mmol) and K₂CO₃ (326 mg, 2.36 mmol) at 25 °C for 6 h and filtered. The filtrate was poured into H₂O (50 mL) and extracted with EtOAc. The organic phase was washed with H₂O and saturated aqueous NaCl, dried Na₂SO₄ and concentrated in vacuo. Flash chromatography afforded **18** as colorless oil (397 mg, yield 61.0%). ¹H NMR (CDCl₃, 400 MHz): δ ppm 7.42 (s, 5H), 7.30 (m, 5H), 6.80 (d, 1H, *J* = 8.0 Hz), 6.66 (s, 1H), 6.59 (d, 1H, *J* = 8.0 Hz), 5.28 (br

d, 1H, $J = 8.4$ Hz), 5.13 (s, 2H), 4.62–4.54 (m, 1H), 3.87 (s, 3H), 3.73 (s, 3H), 3.12–3.04 (m, 2H).

L-3-(3,4-Dihydroxyphenyl)alanine Hydrochloride (19). A solution of **17** (1.93 g, 4.43 mmol) and Pd/C (10%) 31 mg in 20 mL of dry methylene chloride was stirred under hydrogen atmosphere until the starting material disappeared. The catalyst was filtered off and the filtrate was concentrated to afford the crude product, which was dissolved in CH_3CN (250 mL) and 3% Na_2CO_3 (375 mL) and stirred for 15 h, then washed with hexane, acidified with 2 N HCl to pH 3, and extracted with CHCl_3 . The combined organic layers were washed with brine, dried over Na_2SO_4 and evaporated to an oil residue, which was recrystallized from EtOAc/PE to give **19** as white crystal (0.58 g, yield 64%). $[\alpha]_{\text{D}}^{20} = -11.0$ ($c = 1.25$, 1 N HCl) lit.²³ $[\alpha]_{\text{D}}^{20} = -11.3$ ($c = 1.0$, 1 N HCl); Mp 295 °C.

L-3-(3-Methoxy-4-hydroxyphenyl)alanine Hydrochloride (20). Prepared from compound **18** according to the similar procedure to **19**. $[\alpha]_{\text{D}}^{20} = -6.2$ ($c = 1.5$, 1 N HCl) lit³³ $[\alpha]_{\text{D}}^{20} = -5.8$ ($c = 1.0$, 1 N HCl).

N-(9-Fluorenylmethoxycarbonyl)-3,4-dihydroxy-L-phenylalanine (21).²⁴ Compound **19** (1 g, 5 mmol) was dissolved in dioxane-10% Na_2CO_3 (15 mL, 1/2) and the solution stirred on an ice bath 10 min prior to addition of Fmoc-Osu (1.71 g, 5 mmol) in dioxane (5 mL) over 30 min. The reaction was allowed to warm to room temperature and stirred overnight at room temperature. The cream colored suspension was added to a separatory funnel and washed with ether. The aqueous layer was cooled on an ice bath and acidified with 6 N HCl to pH = 3. This aqueous solution was extracted with ethyl acetate. The combined organic layers were washed with brine, and dried over anhydrous Na_2SO_4 . Solvent was removed in vacuo to yield a light brown, foamy solid. The crude Fmoc-DOPA was loaded onto a silica gel column and eluted with $\text{CH}_2\text{Cl}_2/\text{MeOH} = 10/1$ to get N-Fmoc-L-Dopa 1.42 g as white solid in 68% yield. $^1\text{H NMR}$ (DMSO- d_6 , 400 MHz): δ ppm 8.63 (br s, 1H), 8.59 (br s, 1H), 7.87 (d, 2H, $J = 8.0$ Hz), 7.68–7.27 (m, 9H), 6.66–6.51 (m, 3H), 4.21–4.10 (m, 4H), 5.13 (s, 2H), 2.89–2.71 (m, 2H).

3-(3-Methoxy-4-hydroxyphenyl)-2-(9H-fluoren-9-ylmethoxycarbonylamino)-propionic Acid (22). Prepared from compound **20** according to the similar procedure to **21**. The product was used for next step reaction directly.

3-(3,4-Bis-trityloxy-phenyl)-2-(9H-fluoren-9-ylmethoxycarbonylamino)-propionic Acid (23).²⁵ Compound **21** (1 g, 2.5 mmol) and trityl chloride were suspended in 50 mL of anhydrous acetonitrile, and triethylamine (0.7 mL, 5 mmol) was added dropwise. The mixture was stirred at room temperature for 3–5 h, then the solvent was evaporated and the crude product was stirred with 50 mL water and ice. The tan precipitates were filtered, dried and used directly for the next step. $^1\text{H NMR}$ (CHCl_3 , 400 MHz): δ ppm 7.76–7.15 (m, 39H), 7.12 (s, 1H), 7.02 (d, 1H, $J = 8.0$ Hz), 5.59 (d, 1H, $J = 8.0$ Hz), 4.71–4.69 (m, 1H), 4.64–4.19 (m, 3H), 2.89–2.71 (m, 2H).

3-(3-Methoxy-4-trityloxy-phenyl)-2-(9H-fluoren-9-ylmethoxycarbonylamino)-propionic Acid (24). Prepared from compound **22** according to the similar procedure to **23**. $[\alpha]_{\text{D}}^{20} = -27.0$ ($c = 1.3$, DMF); $^1\text{H NMR}$ (CDCl_3 , 400 MHz): δ ppm 7.78–7.12 (m, 25H), 7.02 (d, 1H, $J = 8.0$ Hz), 5.59 (d, 1H, $J = 8.0$ Hz), 4.71–4.69 (m, 1H), 4.64–4.19 (m, 3H), 3.80 (s, 3H), 2.89–2.71 (m, 2H).

(S)-3-(4-Hydroxyphenyl)-2-[(methoxycarbonyl)amino]-1-propanoic Acid, Ethyl Ester (25).²⁶ To a suspension solution of L-tyrosine (5 g, 28 mmol) in 50 mL of methanol was added thionyl chloride (6 mL, 84 mmol) in a dropwise manner at -10 °C. After the addition the solution was allowed warm to room temperature. The reaction mixture was heated at reflux overnight and then concentrated via rotary evaporator to afford the crude ester, which was dissolved in 50 mL of water. The resultant solution was neutralized with NaOH (1.10 g, 28 mmol) before NaHCO_3 (3.5 g, 42 mmol) was added. After the solution was cooled with ice–water, a solution of ethyl chloroformate (2.45 mL, 33 mmol) in 20 mL of CHCl_3 was added. The reaction mixture was stirred for 2 h and then extracted with CHCl_3 . The combined organic layers were

washed with water and dried over Na_2SO_4 . After removal of solvent in vacuo, 6 g (87%) of product was obtained as a pale yellow oil. $[\alpha]_{\text{D}}^{20} = +10.1$ ($c = 1.5$, CHCl_3) lit²⁶ $[\alpha]_{\text{D}}^{18} = +9.3$ ($c = 0.6$, CHCl_3). $^1\text{H NMR}$ (CDCl_3 , 400 MHz): δ ppm 6.98 (d, 2H, $J = 8.4$ Hz), 6.68 (d, 2H, $J = 8.4$ Hz), 5.22 (br d, 1H, $J = 8.0$ Hz), 4.69–4.64 (m, 1H), 4.10 (q, 2H, $J = 7.6$ Hz), 3.80 (s, 3H), 3.10–3.01 (m, 2H), 1.2 (t, 3H, $J = 7.6$ Hz).

(S)-3-(4-Hydroxy-3-nitrophenyl)-2-[(methoxycarbonyl)amino]-1-propanoic Acid, Ethyl Ester (26). NaNO_3 (1.54 g, 18 mmol) and $\text{La}(\text{NO}_3)_3 \cdot 6\text{H}_2\text{O}$ (77.8 mg) were dissolved in 30 mL of 6 N HCl. To this solution was added a solution of **25** (4.84 g, 18.12 mmol) in 60 mL of methylene chloride at 0 °C over 0.5 h. After the addition the solution was warmed to room temperature, and the stirring was continued for 6 h. The organic layer was separated, and the aqueous layer was extracted with methylene chloride. The combined organic layers were washed with water and brine, dried over Na_2SO_4 , and concentrated. The residual oil was chromatographed, eluting with 1/4 ethyl acetate/petroleum ether to afford the product as yellow solid (3.7 g, yield 65%). $^1\text{H NMR}$ (CDCl_3 , 400 MHz): δ ppm 10.5 (d, 1H, $J = 3.2$ Hz), 7.86 (s, 1H), 7.36 (dd, 1H, $^1J = 8.4$ Hz, $^2J = 1.6$ Hz), 7.08 (dd, 1H, $^1J = 8.4$ Hz, $^2J = 1.6$ Hz), 5.20 (br d, 1H, $J = 8.0$ Hz), 4.65–4.62 (m, 1H), 4.17 (q, 2H, $J = 7.6$ Hz), 3.78 (s, 3H), 3.13–3.09 (m, 2H), 1.20 (t, 3H, $J = 7.6$ Hz).

L-3-(3-Nitro-4-hydroxyphenyl)alanine Hydrochloride (27). A mixture of **26** (500 mg, 1.35 mmol) in 10 mL of methanol and 10 mL of 10% KOH was stirred at 50 °C until the starting material disappeared as monitored by TLC. After the solution was neutralized with HCl to pH = 3, it was extracted with ethyl acetate. The organic phase was washed with the brine, dried over Na_2SO_4 , and concentrated in vacuo to afford yellow solid. The solid was recrystallized from EtOH and Et₂O to give L-3-NO₂-tyrosine (212.6 mg, yield 60%). Mp 233–236 °C. $[\alpha]_{\text{D}}^{20} = +3.0$ ($c = 1.0$, 1 N HCl) lit³⁴ $[\alpha]_{\text{D}}^{20} = +4.0$ ($c = 1.0$, 1 N HCl).

3-(3-Nitro-4-hydroxyphenyl)-2-(9H-fluoren-9-ylmethoxycarbonylamino)-propionic Acid (28). Prepared from compound **27** according to the similar procedure to **21**. Yellow foam, yield 80%. $^1\text{H NMR}$ (CDCl_3 , 400 MHz): δ ppm 10.5 (s, 1H), 7.97 (d, 1H, $J = 2.0$ Hz), 7.79–7.27 (m, 9H), 7.04 (d, 1H, $J = 8.4$ Hz), 5.31 (br d, 1H, $J = 8.0$ Hz), 4.66–3.77 (m, 4H), 3.13–2.89 (m, 2H).

2-Amino-3-(4-hydroxy-3-methoxy-phenyl)-propionic Acid (29). A solution of **28** (1 g, 2.2 mmol) and Pd/C (10%) 20 mg in 15 mL of dry methylene chloride was stirred under hydrogen atmosphere until the starting material disappeared. The catalyst was filtered off and the filtrate was concentrated to afford the crude product 0.6 g in yield of 76%. $^1\text{H NMR}$ (CDCl_3 , 400 MHz): δ ppm 7.76–7.29 (m, 9H), 6.61 (d, 1H, $J = 8.0$ Hz), 6.46 (d, 1H, $J = 1.6$ Hz), 6.37 (dd, 1H, $^1J = 8.0$ Hz, $^2J = 1.6$ Hz), 5.31 (br d, 1H, $J = 8.0$ Hz), 4.70–4.60 (m, 1H), 4.50–4.30 (m, 2H), 4.20 (t, 1H, $J = 6.8$ Hz), 3.13–2.89 (m, 2H).

3-(3-Nitro-4-trityloxy-phenyl)-2-(9H-fluoren-9-ylmethoxycarbonylamino)-propionic Acid (30). Prepared from compound **28** according to the similar procedure to **23**. Yellow foam, yield 62%. $^1\text{H NMR}$ (CDCl_3 , 400 MHz): δ ppm 8.02 (d, 1H, $J = 2.0$ Hz), 7.79–7.27 (m, 9H), 7.23–7.08 (m, 16H), 5.31 (br d, 1H, $J = 8.0$ Hz), 4.66–3.77 (m, 4H), 3.13–2.89 (m, 2H). $[\alpha]_{\text{D}}^{20} = -12.0$ ($c = 0.7$, DMF).

3-(3-Tritylamino-4-trityloxy-phenyl)-2-(9H-fluoren-9-ylmethoxycarbonylamino)-propionic Acid (31). Prepared from compound **29** according to the similar procedure to **21**. White foam, yield 56%. $^1\text{H NMR}$ (CDCl_3 , 400 MHz): δ ppm 7.80–7.30 (m, 8H), 7.20–7.00 (m, 31H), 6.71–6.69 (dd, 2H, $^1J = 8.4$ Hz, $^2J = 1.5$ Hz), 5.20 (d, 1H, $J = 8.4$ Hz), 4.60–4.50 (m, 1H), 4.40–4.30 (m, 2H), 4.22 (t, 1H, $J = 6.8$ Hz), 3.22–2.93 (m, 2H); EI-MS m/z (%): 416 (M – 2Trt, 6), 238 (M – 2Trt-Fmoc, 14), 243 (Trt, 100). $[\alpha]_{\text{D}}^{20} = -3.0$ ($c = 1.3$, DMF).

N-[(1,1-Dimethylethoxy)carbonyl]-3-(3-formyl-4-hydroxyphenyl)-L-alanine (32).²⁷ Powdered sodium hydroxide (1.71 g, 42.72 mmol) was added to a suspension of *N*-Boc-L-tyrosine (2 g, 7.12 mmol) in water (0.256 mL, 14.13 mmol), and chloroform (30 mL). The mixture was refluxed for 4 h. Additional sodium hydroxide

was added (0.84 g, 21.36 mmol) in two portions after 1 and 1.5 h, respectively. The reaction was then diluted with water and ethyl acetate, and the aqueous layer was acidified to pH 1 with 1 N HCl and extracted with ethyl acetate. The organic extracts were washed with brine, dried over Na₂SO₄, and concentrated. Flash column chromatography (silica gel, 12/1 CHCl₃/MeOH 1% acetic acid as eluent) afforded the desired product **32** as a brown oil (0.72 g, 33%) and recovered starting material 0.62 g. ¹H NMR (CDCl₃, 400 MHz): δ ppm 10.92 (s, 1H), 9.84 (s, 1H), 7.37 (d, 1H, *J* = 1.6 Hz), 7.33 (d, 1H, *J* = 8.4 Hz), 6.74 (d, 1H, *J* = 7.8 Hz), 5.28 (d, 1H, *J* = 8.0 Hz), 5.01–4.94 (m, 1H), 3.06–3.03 (m, 2H), 1.40 (s, 9H).

L-3-(3-Formyl-4-(benzyloxy)phenyl)-N-(9-fluorenylmethoxycarbonyl)alanine Benzyl Ester (33). Compound **32** (600 mg, 1.94 mmol) was dissolved in 10 mL 20% TFA in DCM, the solution was stirred at room temperature for 30 min. Then the solvent was evaporated. The residue was dissolved in 10% Na₂CO₃ (10 mL) and a solution of FmocOSu (786 mg, 2.3 mmol) in dioxane (10 mL) was added dropwise. The mixture was stirred at room temperature overnight, then poured into water and extracted with diethyl ether. The aqueous phase was acidified with 1 N HCl to pH 3, and the aqueous phase was extracted with EtOAc. After usual workup, the residue was dissolved in 10 mL DMF, BnBr (0.56 mL, 4.64 mmol), K₂CO₃ (640 mg, 4.64 mmol), n-Bu₄NI (81 mg, 0.125 mmol) were added. The mixture was stirred at room temperature overnight. Then, the reaction mixture was poured into water and extracted with diethyl ether. The organic phase was dried over Na₂SO₄, and the solvent was removed in vacuo. Flash column chromatography (silica gel, 1/4 EtOAc/PE as eluent) afforded the desired product **33** as a white foam (110 mg, 51%). ¹H NMR (CDCl₃, 400 MHz): δ ppm 10.49 (s, 1H), 7.77–7.26 (m, 19H), 7.16 (d, 1H, *J* = 8.4 Hz), 6.87 (d, 1H, *J* = 8.4 Hz), 5.39–5.33 (m, 1H), 5.18 (s, 2H), 5.14 (s, 2H), 4.70–4.64 (m, 1H), 4.45–4.11 (m, 3H), 3.13–3.04 (m, 2H). EIMS: *m/z* 611 (M⁺), 178 (100), 91 (24). [α]_D²² = +3.2 (*c* = 1.7, CHCl₃).

L-3-[3-(tert-Butoxycarbonyl)-4-(benzyloxy)phenyl]-N-(9-fluorenylmethoxycarbonyl)alanine Benzyl Ester (34). Compound **33** (220 mg, 0.45 mmol) was added to a stirred suspension of Ag₂O (158 mg, 0.68 mmol) in 4 mL of 5% NaOH aq. After being stirred for 24 h, the suspension was filtered and the solid was washed with H₂O. The filtrate was cooled at 0 °C, acidified with 1 N HCl and extracted with Et₂O. Drying and concentrated for next use. The crude product, *tert*-butyl 2,2,2-trichloroacetimidate (398 mg, 1.35 mmol) was dissolved in 10 mL of dry THF. 50 μL of BF₃·Et₂O was added to the solution. The solution was stirred at room temperature for 16 h before concentrated. The residue was then diluted with saturated NaHCO₃ and ethyl acetate, and the aqueous layer was back-extracted with ethyl acetate. The organic extracts were washed with H₂O, brine, dried over Na₂SO₄, and concentrated. Flash column chromatography (silica gel, 6/1 PE/EtOAc) afforded the desired product **34** as a white solid (150 mg, 61%). ¹H NMR (CDCl₃, 400 MHz): δ ppm 7.76–7.26 (m, 19H), 7.16 (d, 1H, *J* = 8.4 Hz), 6.87 (d, 1H, *J* = 8.4 Hz), 5.39–5.33 (m, 1H), 5.18 (s, 2H), 5.14 (s, 2H), 4.72–4.10 (m, 4H), 3.13–3.04 (m, 2H), 1.50 (s, 9H).

L-3-[3-(tert-Butoxycarbonyl)-4-(tert-butoxycarbonyl)phenyl]-N-(9-fluorenylmethoxycarbonyl)alanine Benzyl Ester (35). 10% Pd–C (10 mg) and **34** (320 mg, 0.46 mmol) was dissolved in 10 mL of dry EtOH. The solution was treated with H₂ and stirred at room temperature overnight. Pd–C was filtered and the filtrate was concentrated in vacuo to afford colorless oil. Then, the oil (181 mg, 0.36 mmol), Boc₂O (156 mg, 0.72 mmol), Et₃N (20 mL) and catalytic amount of DMAP were dissolved in 18 mL of DCM. The solution was stirred at room temperature for 2 h. Then the solvent was removed in vacuo. Flash column chromatography (silica gel, 1/4 EtOAc/PE as eluent) afforded the desired product **35** as a white foam (110 mg, 51% yield). ¹H NMR (CDCl₃, 400 MHz): δ 7.76–7.26 (m, 8H), 7.18–7.02 (m, 3H), 5.59 (br d, 1H, *J* = 8.0 Hz), 4.74–4.69 (m, 1H), 4.64–4.18 (m, 3H), 3.21–3.13 (m, 2H), 1.56 (s, 9H), 1.49 (s, 9H). ESIMS: *m/z* 602 (M – H)[–], 546 (M – ^tBu), 530 (M – O^tBu). [α]_D²² = +19.8 (*c* = 0.5, CHCl₃). Anal. Calcd

for C₃₄H₃₇NO₉: C, 67.65; H, 6.18; N, 2.32. Found: C, 67.76; H, 6.37; N, 2.06.

Cyclo-(CH₂-CO-Adi-Leu-Tyr-Ac6c-Asn-Ava-Cys)-amide (peptide 4a). ESI-MS, *m/z*: calc. 916.1 (M – H)[–], found 916.5. *t*_R = 16.2 min (10–70% of solvent B in 30 min, purity 99%); *t*_R = 24.6 min (10–70% of solvent C in 30 min, purity 95%).

Cyclo-(CH₂-CO-Adi-Leu-Tyr-Ac6c-Asn-Ava-Cys (O))-amide (R) (peptide 4b). ESI-MS, *m/z*: calc. 932.1 (M – H)[–], found 932.3. *t*_R = 15.0 min (10–70% of solvent B in 30 min, purity 98%); *t*_R = 20.9 min (10–70% of solvent C in 30 min, purity 97%).

Cyclo-(CH₂-CO-Adi-Leu-Tyr-Ac6c-Asn-Ava-Cys (O))-amide (S) (peptide 4c). ESI-MS, *m/z*: calc. 956.1 (M + Na)⁺, found 956.4. *t*_R = 15.0 min (10–70% of solvent B in 30 min, purity 98%); *t*_R = 21.0 min (10–70% of solvent C in 30 min, purity 97%).

Cyclo-(CH₂-CO-Adi-Leu-(3'-OH-Tyr)-Ac6c-Asn-Ava-Cys)-amide (peptide 5a). ESI-MS, *m/z*: calc. 956.1 (M + Na)⁺, found 956.3. *t*_R = 14.7 min (10–70% of solvent B in 30 min, purity 99%); *t*_R = 21.7 min (10–70% of solvent C in 30 min, purity 99%).

Cyclo-(CH₂-CO-Adi-Leu-(3'-OH-Tyr)-Ac6c-Asn-Ava-Cys (O))-amide (R) (peptide 5b). ESI-MS, *m/z*: calc. 948.1 (M – H)[–], found 948.3. *t*_R = 14.8 min (10–70% of solvent B in 30 min, purity 95%); *t*_R = 22.5 min (10–70% of solvent C in 30 min, purity 95%).

Cyclo-(CH₂-CO-Adi-Leu-(3'-OH-Tyr)-Ac6c-Asn-Ava-Cys (O))-amide (S) (peptide 5c). ESI-MS, *m/z*: calc. 948.1 (M – H)[–], found 948.3. *t*_R = 15.3 min (10–70% of solvent B in 30 min, purity 95%); *t*_R = 22.6 min (10–70% of solvent C in 30 min, purity 95%).

Cyclo-(CH₂-CO-Adi-Leu-(3'-OMe-Tyr)-Ac6c-Asn-Ava-Cys)-amide (peptide 6a). ESI-MS, *m/z*: calc. 948.1 (M + H)⁺, found 948.2. *t*_R = 15.0 min (10–70% of solvent B in 30 min, purity 97%); *t*_R = 21.2 min (10–70% of solvent C in 30 min, purity 96%).

Cyclo-(CH₂-CO-Adi-Leu-(3'-OMe-Tyr)-Ac6c-Asn-Ava-Cys (O))-amide (R) (peptide 6b). ESI-MS, *m/z*: calc. 964.1 (M + H)⁺, found 964.3. *t*_R = 15.3 min (10–70% of solvent B in 30 min, purity 99%); *t*_R = 22.6 min (10–70% of solvent C in 30 min, purity 97%).

Cyclo-(CH₂-CO-Adi-Leu-(3'-OMe-Tyr)-Ac6c-Asn-Ava-Cys (O))-amide (S) (peptide 6c). ESI-MS, *m/z*: calc. 964.1 (M + H)⁺, found 964.3. *t*_R = 15.8 min (10–70% of solvent B in 30 min, purity 99%); *t*_R = 22.8 min (10–70% of solvent C in 30 min, purity 99%).

Cyclo-(CH₂-CO-Adi-Leu-(3'-NH₂-Tyr)-Ac6c-Asn-Ava-Cys)-amide (peptide 7a). ESI-MS, *m/z*: calc. 932.1 (M⁺), found 932.4. *t*_R = 15.7 min (10–70% of solvent B in 30 min, purity 99%); *t*_R = 21.3 min (10–70% of solvent C in 30 min, purity 99%).

Cyclo-(CH₂-CO-Adi-Leu-(3'-NH₂-Tyr)-Ac6c-Asn-Ava-Cys (O))-amide (R) (peptide 7b). ESI-MS, *m/z*: calc. 947.1 (M – H)[–], found 947.3. *t*_R = 14.4 min (10–70% of solvent B in 30 min, purity 96%); *t*_R = 20.2 min (10–70% of solvent C in 30 min, purity 97%).

Cyclo-(CH₂-CO-Adi-Leu-(3'-NH₂-Tyr)-Ac6c-Asn-Ava-Cys (O))-amide (S) (peptide 7c). ESI-MS, *m/z*: calc. 971.1 (M + Na)⁺, found 971.5. *t*_R = 15.0 min (10–70% of solvent B in 30 min, purity 99%); *t*_R = 21.2 min (10–70% of solvent C in 30 min, purity 97%).

Cyclo-(CH₂-CO-Adi-Leu-(3'-NO₂-Tyr)-Ac6c-Asn-Ava-Cys)-amide (peptide 8a). ESI-MS, *m/z*: calc. 961.1 (M – H)[–], found 961.1. *t*_R = 15.1 min (10–70% of solvent B in 30 min, purity 98%); *t*_R = 21.6 min (10–70% of solvent C in 30 min, purity 97%).

Cyclo-(CH₂-CO-Adi-Leu-(3'-NO₂-Tyr)-Ac6c-Asn-Ava-Cys (O))-amide (R) (peptide 8b). ESI-MS, *m/z*: calc. 1001.1 (M + Na)⁺, found 1001.1. *t*_R = 13.9 min (10–70% of solvent B in 30 min, purity 96%); *t*_R = 22.4 min (10–70% of solvent C in 30 min, purity 95%).

Cyclo-(CH₂-CO-Adi-Leu-(3'-NO₂-Tyr)-Ac6c-Asn-Ava-Cys (O))-amide (S) (peptide 8c). ESI-MS, *m/z*: calc. 977.1 (M – H)[–], found 977.3. *t*_R = 13.9 min (10–70% of solvent B in 30 min, purity 98%); *t*_R = 22.4 min (10–70% of solvent C in 30 min, purity 98%).

Cyclo-(CH₂-CO-Adi-Leu-(3'-CO₂H-Tyr)-Ac6c-Asn-Ava-Cys)-amide (peptide 9a). ESI-MS, *m/z*: calc. 962.1 (M + H)⁺, found 962.1. *t*_R = 15.7 min (10–70% of solvent B in 30 min, purity 99%); *t*_R = 21.9 min (10–70% of solvent C in 30 min, purity 96%).

Cyclo-(CH₂-CO-Adi-Leu-(3'-CO₂H-Tyr)-Ac6c-Asn-Ava-Cys (O))-amide (R) (peptide 9b). ESI-MS, *m/z*: calc. 978.1 (M +

H)⁺, found 978.3. $t_R = 15.1$ min (10–70% of solvent B in 30 min, purity 98%); $t_R = 21.6$ min (10–70% of solvent C in 30 min, purity 97%).

Cyclo-(CH₂-CO-Adi-Leu-(3'-CO₂H-Tyr)-Ac6c-Asn-Ava-Cys (O))-amide (S) (peptide 9c). ESI-MS, m/z : calc. 978.1 (M + H)⁺, found 978.1. $t_R = 15.1$ min (10–70% of solvent B in 30 min, purity 98%); $t_R = 22.6$ min (10–70% of solvent C in 30 min, purity 99%).

Cyclo-(CH₂-CO-Gla-Leu-(3'-NH₂-Tyr)-Ac6c-Asn-Ava-Cys)-amide (peptide 10a). ESI-MS, m/z : calc. 1001.2 (M + K)⁺, found 1001.3. $t_R = 16.2$ min (10–70% of solvent B in 30 min, purity 98%); $t_R = 24.3$ min (10–70% of solvent C in 30 min, purity 97%).

Cyclo-(CH₂-CO-Gla-Leu-(3'-NH₂-Tyr)-Ac6c-Asn-Ava-Cys (O))-amide (R) (peptide 10b). ESI-MS, m/z : calc. 977.1 (M – H)[–], found 977.1. $t_R = 15.7$ min (10–70% of solvent B in 30 min, purity 99%); $t_R = 23.8$ min (10–70% of solvent C in 30 min, purity 97%).

Cyclo-(CH₂-CO-Gla-Leu-(3'-NH₂-Tyr)-Ac6c-Asn-Ava-Cys (O))-amide (S) (peptide 10c). ESI-MS, m/z : calc. 977.1 (M – H)[–], found 977.3. $t_R = 15.9$ min (10–70% of solvent B in 30 min, purity 96%); $t_R = 23.8$ min (10–70% of solvent C in 30 min, purity 95%).

Cyclo-(CH₂-CO-Gla-Leu-(3'-NH₂-Tyr)-Ac6c-Asn-β-Ala-Cys)-amide (peptide 11a). ESI-MS, m/z : calc. 919.0 (M – H)[–], found 918.4. $t_R = 15.7$ min (10–70% of solvent B in 30 min, purity 99%); $t_R = 22.4$ min (10–70% of solvent C in 30 min, purity 99%).

Cyclo-(CH₂-CO-Gla-Leu-(3'-NH₂-Tyr)-Ac6c-Asn-β-Ala-Cys (O))-amide (R) (peptide 11b). ESI-MS, m/z : calc. 935.0 (M – H)[–], found 934.3. $t_R = 15.7$ min (10–70% of solvent B in 30 min, purity 98%); $t_R = 23.7$ min (10–70% of solvent C in 30 min, purity 96%).

Cyclo-(CH₂-CO-Gla-Leu-(3'-NH₂-Tyr)-Ac6c-Asn-β-Ala-Cys (O))-amide (S) (peptide 11c). ESI-MS, m/z : calc. 935.0 (M – H)[–], found 934.3. $t_R = 15.7$ min (10–70% of solvent B in 30 min, purity 98%); $t_R = 24.3$ min (10–70% of solvent C in 30 min, purity 99%).

Cyclo-(CH₂-CO-Gla-Leu-(3'-NH₂-Tyr)-Ac6c-Asn –Cys)-amide (peptide 12a). ESI-MS, m/z : calc. 963.0 (M – H)[–], found 962.3. $t_R = 15.6$ min (10–70% of solvent B in 30 min, purity 99%); $t_R = 22.4$ min (10–70% of solvent C in 30 min, purity 98%).

Cyclo-(CH₂-CO-Gla-Leu-(3'-NH₂-Tyr)-Ac6c-Asn-Cys (O))-amide (R) (peptide 12b). ESI-MS, m/z : calc. 878.8 (M⁺), found 878.3. $t_R = 14.9$ min (10–70% of solvent B in 30 min, purity 99%); $t_R = 23.5$ min (10–70% of solvent C in 30 min, purity 95%).

Cyclo-(CH₂-CO-Gla-Leu-(3'-NH₂-Tyr)-Ac6c-Asn-Cys (O))-amide (S) (peptide 12c). ESI-MS, m/z : calc. 878.8 (M⁺), found 878.3. $t_R = 15.1$ min (10–70% of solvent B in 30 min, purity 99%); $t_R = 24.2$ min (10–70% of solvent C in 30 min, purity 97%).

Acknowledgment. Appreciation is expressed to Prof. Xu Shen and his colleagues of the DDDC at SIMM for their kind assistance with the Biacore 3000 instrument. The authors are also thankful for Dr. Marc C. Nicklaus of LMC at NCI for his helpful advise with the molecular modeling. This work was financially supported in part by Chinese Academy of Sciences (No. KSCX1-S.W.-11) and Ministry of Science and Technology of China (No. 2004CB518903), and in part by the intramural research program of the National Cancer Institute, National Institutes of Health (No. NO1-CO-12400).

References

- Pawson, T.; Gish, G. D.; Nash, P. SH2 domains, interaction modules and cellular wiring. *Trends Cell Biol.* **2001**, *11*, 504–511.
- Pawson, T. Specificity in signal transduction: From phosphotyrosine-SH2 domain interactions to complex cellular systems. *Cell* **2004**, *116*, 191–203.
- Yip, S. S.; Daly, R. J. Up-regulation of the protein tyrosine phosphatase SHP-1 in human breast cancer and correlation with GRB2 expression. *Int. J. Cancer* **2000**, *88*, 363–368.
- Lim, S. J.; Lopez-Berestein, G.; Hung, M. C.; Lupu, R.; Tari, A. M. Grb2 downregulation leads to Akt inactivation in heregulin-stimulated and ErbB2-overexpressing breast cancer cells. *Oncogene* **2000**, *19*, 6271–6276.
- Machida, K.; Mayer, B. J. The SH2 domain: versatile signaling module and pharmaceutical target. *BBA-Proteins Proteomics* **2005**, *1747*, 1–25.
- Muller, G. Peptidomimetic SH2 domain antagonists for targeting signal transduction. *Top. Curr. Chem.* **2001**, *211*, 17–59.
- Fretz, H.; Furet, P.; Garcia-Echeverria, C.; Rahuel, J.; Schoepfer, J. Structure-based design of compounds inhibiting Grb2-SH2 mediated protein–protein interactions in signal transduction pathways. *Curr. Pharm. Des.* **2000**, *6*, 1777–1796.
- Shi, Z.-D.; Lee, K.; Liu, H.; Zhang, M.; Roberts, L. R.; Worthy, K. M.; Fivash, M. J.; Fisher, R. J.; Yang, D.; Burke, T. R., Jr. A novel macrocyclic tetrapeptide mimetic that exhibits low-picomolar Grb2 SH2 domain-binding affinity. *Biochem. Biophys. Res. Commun.* **2003**, *310*, 378–383.
- Shakespeare, W.; Yang, M.; Bohacek, R.; Cerasoli, F.; Stebbins, K.; Sundaramoorthi, R.; Azimioara, M.; Vu, C.; Pradeepan, S.; Metcalf, C., III; Haraldson, C.; Merry, T.; Dalgarno, D.; Narula, S.; Hatada, M.; Lu, X.; Van Schravendijk, M. R.; Adams, S.; Violette, S.; Smith, J.; Guan, W.; Bartlett, C.; Herson, J.; Iulucci, J.; Weigele, M.; Sawyer, T. Structure-based design of an osteoclast-selective, non-peptide Src homology 2 inhibitor with in vivo antiresorptive activity. *Proc. Natl. Acad. Sci. U.S.A.* **2000**, *97*, 9373–9378.
- Liu, W.-Q.; Vidal, M.; Olszowy, C.; Million, E.; Lenoir, C.; Dhôtel, H. and Garbay, C. Structure–activity relationships of small phosphopeptides, inhibitors of Grb2-SH2 domain, and their prodrugs. *J. Med. Chem.* **2004**, *47*, 1223–1233.
- Gay, B.; Suarez, S.; Caravatti, G.; Furet, P.; Meyer, T.; Schoepfer, J. Selective GRB2 SH2 inhibitors as anti-Ras therapy. *Int. J. Cancer* **1999**, *83*, 235–241.
- Bradshaw, J. M.; Waksman, G. Molecular recognition by SH2 domains. *Adv. Protein Chem.* **2003**, *61*, 161–210.
- Shakespeare, W. C. SH2 domain inhibition: a problem solved? *Curr. Opin. Chem. Biol.* **2001**, *5*, 409–415.
- Oligino, L.; Lung, F.-D. T.; Sastry, L.; Bigelow, J.; Cao, T.; Curran, M.; Burke, T. R., Jr.; Wang, S.; Krag, D.; Roller, P. P.; King, C. R. Nonphosphorylated peptide ligands for the Grb2 Src homology 2 domain. *J. Biol. Chem.* **1997**, *272*, 29046–29052.
- Long, Y.-Q.; Voigt, J. H.; Lung, F.-D. T.; King, C. R.; Roller, P. P. Significant compensatory role of position Y-2 conferring high affinity to non phosphorylated inhibitors of GRB2–SH2 domain. *Bioorg. Med. Chem. Lett.* **1999**, *9*, 2267–2272.
- Long, Y.-Q.; Yao, Z.-J.; Voigt, J. H.; Lung, F.-D. T.; Luo, J. H.; Burke, T. R., Jr.; King, C. R.; Yang, D.-J.; Roller, P. P. Structural requirements for Tyr in the consensus sequence Y–E–N of a novel nonphosphorylated inhibitor to the Grb2-SH2 domain. *Biochem. Biophys. Res. Commun.* **1999**, *264*, 902–908.
- Li, P.; Zhang, M.; Long, Y.-Q.; Peach, M. L.; Liu, H.; Yang, D.; Nicklaus, M.; Roller, P. P. Potent Grb2-SH2 domain antagonists not relying on phosphotyrosine mimics. *Bioorg. Med. Chem. Lett.* **2003**, *13*, 2173–2177.
- Long, Y.-Q.; Guo, R.; Luo, J. H.; Yang, D.; Roller, P. P. *Biochem. Biophys. Res. Commun.* **2003**, *310*, 334–340.
- Li, P.; Zhang, M.; Peach, M. L.; Zhang, X.; Liu, H.; Nicklaus, M.; Yang, D.; Roller, P. P. Structural basis for a non-phosphorus-containing cyclic peptide binding to Grb2-SH2 domain with high affinity. *Biochem. Biophys. Res. Commun.* **2003**, *307*, 1038–1044.
- Long, Y.-Q.; Lung, F.-D. T.; Roller, P. P. Global optimization of conformational constraint on nonphosphorylated cyclic peptide antagonists of the Grb2-SH2 domain. *Bioorg. Med. Chem.* **2003**, *11*, 3929–3936.
- Rahuel, J.; Gay, B.; Erdmann, D.; Strauss, A.; GarciaEcheverria, C.; Furet, P.; Caravatti, G.; Fretz, H.; Schoepfer, J.; Grutter, M. G. Structural basis for specificity of Grb2-SH2 revealed by a novel ligand binding mode. *Nature Struct. Biol.* **1996**, *3*, 586–589.
- Boger, D. L.; Yohannes, D. Selectively protected L-Dopa derivatives: application of the benzylic hydroperoxide rearrangement. *J. Org. Chem.* **1987**, *52*, 5283–5286.
- Boger, D. L.; Zhou, J. Total synthesis of (+)-Piperazinomycin. *J. Am. Chem. Soc.* **1993**, *115*, 11426–11433.
- Sever, M. J.; Wilker, J. J. Synthesis of peptides containing DOPA 3,4-dihydroxy phenylalanine. *Tetrahedron* **2001**, *57*, 29; 6139–6146.
- Mastrolorenzo, A.; Scozzafava, A.; Supuran, C. T. 4-Toluenesulfonylureido derivatives of amines, amino acids and dipeptides: a novel class of potential antitumor agents. *Eur. J. Pharm. Sci.* **2000**, *11*, 325–332.
- Ma, D.; Tang, W.; Kozikowski, A. P.; Lewin, N. E.; Blumberg, P. M. General and Stereospecific Route to 9-Substituted, 8,9-Disubstituted, and 9, 10-Disubstituted Analogues of Benzolactam-V8. *J. Org. Chem.* **1999**, *64*, (17), 6366–6373.

- (27) Jung, M. E.; Lazarova, T. I. Efficient Synthesis of Selectively Protected L-Dopa Derivatives from L-Tyrosine via Reimer-Tiemann and Dakin Reactions. *J. Org. Chem.* **1997**, *62* (5), 1553–1555.
- (28) Song, Y.-L.; Roller, P. P.; Long, Y.-Q. Development of L-3-aminotyrosine suitably protected for the synthesis of a novel nonphosphorylated hexapeptide with low-nanomolar Grb2-SH2 domain-binding affinity. *Bioorg. Med. Chem. Lett.* **2004**, *14*, 3205–3208.
- (29) Sastry, L.; Cao, T.; King, R. Multiple Grb2-protein complexes in human cancer cells. *Int. J. Cancer* **1997**, *70*, 208–213.
- (30) Schrödinger Inc. (www.schrodinger.com)
- (31) Kaminski, G. A.; Friesner, R. A.; Tirado-Rives, J.; Jorgensen, W. L. Evaluation and reparametrization of the OPLS-AA force field for proteins via comparison with accurate quantum chemical calculations on peptides. *J. Phys. Chem. B* **2001**, *105*, 6474–6487.
- (32) Ryckaert, J. P.; Ciccotti, G.; Berendsen, H. J. C. Numerical integration of the Cartesian equations of motion of a system with constraints: molecular dynamics of *n*-alkanes. *J. Comput. Phys.* **1977**, *23*, 327–341.
- (33) Chem Abstr 79; 105578.
- (34) *Beil.* **14**(2), 397.
JM050910X